Nanostructures

DOI: 10.1002/ange.200700234

Boron Nitride Nanomesh: Functionality from a Corrugated Monolayer**

*Simon Berner, Martina Corso, Roland Widmer, Oliver Groening, Robert Laskowski, Peter Blaha, Karlheinz Schwarz, Andrii Goriachko, Herbert Over, Stefan Gsell, Matthias Schreck, Hermann Sachdev, Thomas Greber, and Jürg Osterwalder**

An important challenge in nanoscience and nanotechnology is the immobilization of small entities in regular two-dimensional arrays on surfaces. Visionary concepts such as molecular electronics, molecular or ultrasmall magnetic memory cells, and quantum computers, but also highly selective catalysts and functional surfaces, are based on this approach. The array dimensions must be far below 100 nm, where lithographic methods are no longer applicable. Therefore, research focuses on nanotemplates that form over macroscopically large areas by self-assembly, and which can trap molecules or lead to the nucleation of ultrasmall metallic clusters.[1]

Recently, an intriguing superstructure was reported in atomically thin films of hexagonal boron nitride (h-BN) on Rh(111).[2] Decomposition of borazine $(HBNH)_3$ precursor molecules on the hot rhodium surface leads to spontaneous formation of a highly regular hexagonal structure with a periodicity of 3.22 nm and the appearance of a mesh with pores of about 2 nm in diameter. The periodicity of 3.22 nm was recently confirmed by surface X-ray diffraction experiments; it corresponds to a coincidence lattice of (13×13) h-BN units on (12×12) Rh lattice spacings.[3] Neither the detailed atomic structure of the boron nitride nanomesh on Rh(111) nor the mechanism leading to this large-scale self-assembly is fully understood, except for the conjecture that the lattice mismatch is an important but not the only factor: the h-BN lattice constant is 6.7% smaller than that of Rh(111). The knowledge of the atomic structure is a prerequisite for further functionalization of the nanomesh and will open the way for rational design of templates for a variety of nanoscopic entities.

A very similar nanomesh was observed on Ru(0001),[4] with roughly the same periodicity and pore size, in line with a similar lattice mismatch of h-BN as on Rh(111). In the context of this study, a structural model different from that in reference [2] was discussed for both systems that turned out to be also consistent with the entirety of all experimental data available. Instead of two mesh layers,[2] this new model consists of a single but complete layer that is strongly corrugated. Recent density functional theory (DFT) calculations[5] provide further support for the possible single-layer character of the boron nitride nanomesh. Its suitability as a general-purpose template for the formation of supramolecular structures should therefore be questioned. Here we present conclusive experimental evidence for its single-layer character and demonstrate that the edges of the pores form strong confining potentials for trapping molecules well above room temperature.

Low-temperature scanning tunneling microscopy (STM) images recorded at 77 K with small sample bias voltages to image states near the Fermi level allow the atomic structure inside the mesh pores or on the wires to be resolved. Figure 1a presents an example in which a few nanomesh unit cells can be distinguished. The atomic corrugation has the periodicity of the single h-BN unit cells and is thus due to only one atomic species. In the related case of Ni(111), on which a simple (1×1) overlayer of h-BN is formed,[6] DFT calculations showed that under these conditions STM images the N atoms as bright protrusions.[7] This is likely the case also on Rh(111). On top of this atomic corrugation, the image is modulated with the nanomesh periodicity: the rims around the pores are highlighted, while the pores and the inner parts of the wires appear darker.[8] This large-scale modulation can be removed by filtering the corresponding Fourier coefficients from the image (Figure 1b and d). Instead of the round nanomesh pores, the image is now dominated by asymmetric

[*] Dr. S. Berner,[+] Dr. M. Corso,[+] Prof. Dr. T. Greber, Prof. Dr. J. Osterwalder
Physik-Institut, Universität Zürich
Winterthurerstrasse 190, 8057 Zürich (Switzerland)
Fax: (+41) 446-355-704
E-mail: osterwal@physik.uzh.ch
Homepage: http://www.nanomesh.ch
Dr. R. Widmer, Dr. O. Groening
EMPA Swiss Federal Laboratories for Materials Testing and Research, 3602 Thun (Switzerland)
Dr. R. Laskowski, Prof. Dr. P. Blaha, Prof. Dr. K. Schwarz
Institut für Materialchemie, Technische Universität Wien
1060 Vienna (Austria)
Dr. A. Goriachko, Prof. Dr. H. Over
Institut für Physikalische Chemie, Justus-Liebig-Universität Giessen
35392 Giessen (Germany)
S. Gsell, Dr. M. Schreck
Institut für Physik, Universität Augsburg
86135 Augsburg (Germany)
Dr. H. Sachdev
Allgemeine und Anorganische Chemie FR 8.1
Universität des Saarlandes, 66041 Saarbrücken (Germany)

[+] These authors contributed equally to this work.

[**] We thank Martin Klöckner for expert technical assistance. Supported by the European Commission under the contract NMP4-CT-2004-013817 "NanoMesh", and by the Swiss National Science Foundation under the contract 200020-107783.

Supporting information for this article is available on the WWW under http://www.angewandte.org or from the author.

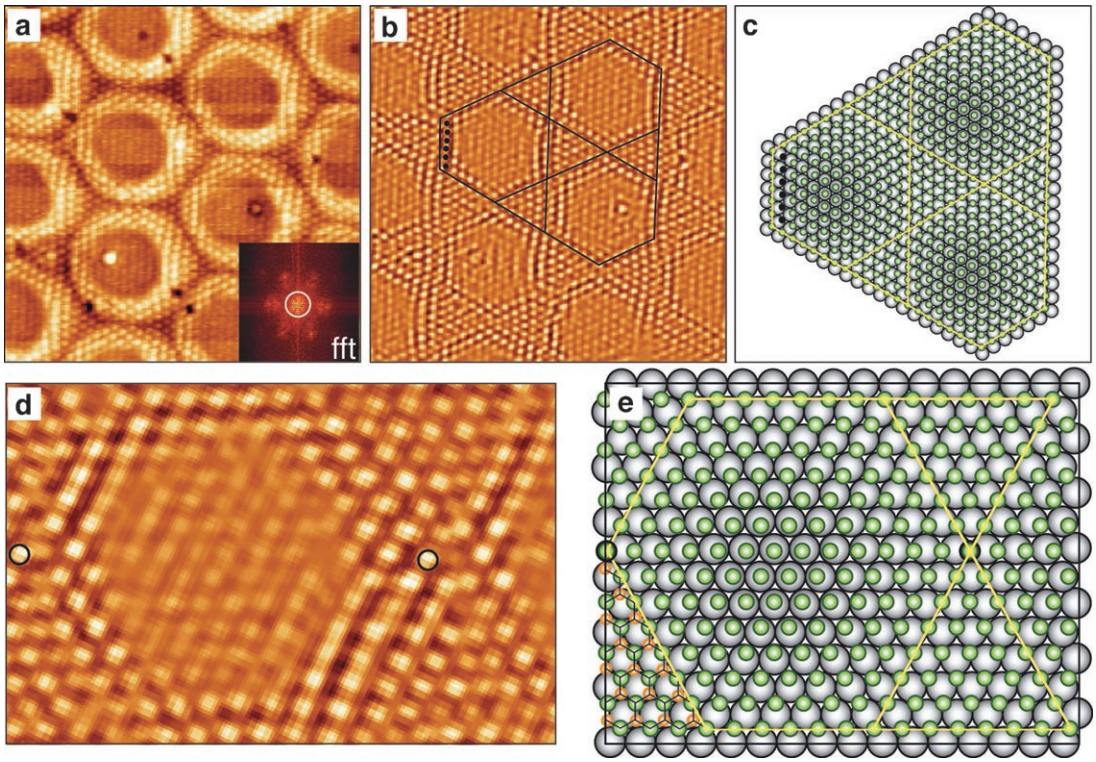

Figure 1. Atomic structure of the nanomesh. a) Constant-current STM image taken at 77 K in which the h-BN nanomesh is atomically resolved (9.4×9.4 nm^2, $I_t = 1$ nA, $V_s = -2$ mV). Only one atomic species is imaged. In (b), image (a) has been filtered in order to remove the 3.22-nm nanomesh periodicity and to emphasize the atomic corrugation in the wires and pores. For this filtering, the six spots inside the white circle around (0,0) in the fast Fourier transform (FFT) image of (a), shown in the inset, have been removed. c) Atomic model for the single-layer nanomesh representing the N atoms (green spheres) for the area delimited by the black lines in (b). The N atoms form a laterally rigid hexagonal lattice, and therefore the misfit with the Rh(111) substrate is uniformly distributed. d) and e) zoomed views of (b) and (c) for better visibility and for permitting atom counting within the unit cell. Some complete h-BN units are shown at the bottom left of (e). Orange spheres are B atoms.

hexagons that define their rims. They are surrounded by triangular areas that form the mesh wires. The image contains enough detail to produce from it the atomic model given in Figure 1c and e. A single nanomesh unit cell is formed by 169 N atoms (and 169 B atoms, not visible in the STM images). The sides of an asymmetric hexagon are formed by rows of N atoms containing alternating 6 or 7 N–N spacings. Each hexagon is bordered by six equilateral triangles with sizes defined by the corresponding side of the hexagon. Each pair of neighboring triangles shares an N atom which defines the center of the nanomesh wire. These structural elements generate the (13×13) periodicity of the nanomesh. Around the centers of the hexagons, over an area roughly equal to the size of the pores, the hexagonal atomic lattice is unperturbed. However, near the rim of the hexagons, the atomic rows appear curved and lead to a wavy nature of the atomic rows along the mesh wires.[9] Most importantly, these images clearly show that the atomic lattice is continuous, also in the transition region from mesh wires to pores, which rules out the steplike topography that would occur in the original two-layer model.

Density functional calculations for h-BN on Ni(111)[7] and later also on Rh(111)[5] have shown that h-BN is bonded only if B sits near a face-centered cubic (fcc) or hexagonal close-packed (hcp) hollow site and N is close to the on-top position with regard to the surface metal atoms. Other sites for h-BN on the transition metal surface are not stable at all. Due to the strong lattice mismatch of h-BN on Rh(111), a rigid boron nitride layer offers such sites favorable for bonding only in a small area of the (13×13) unit cell (Figure 1c and e). These areas are responsible for bonding of the mesh layer to the substrate, while other areas of the mesh may be even repelled from the surface and are bound only due to the strong cohesive forces within the h-BN film itself. We argue that the pores seen in the STM images are mainly due to the area where h-BN occupies nearly the (hollow, on-top) positions for (B, N), respectively. The observed pore diameter of 2 nm corresponds to roughly 8 N–N spacings over which this strong bonding is maintained.

Laskowski et al.[5] simulated the nanomesh unit cell within an ab initio force-field approach, and the equilibrium structure that they found confirms the general picture that emerges from the low-temperature STM images. The combination of dominant in-plane cohesive forces and a strongly modulated substrate/film force field makes the h-BN nanomesh a rather unique system, with an intralayer lattice constant close to that of unstrained bulk boron nitride[2] and a film corrugation close to 0.55 Å, as suggested by the DFT calculations.[5] Examples of nanotemplates in the literature are often based on strain-relief patterns such as those observed in epitaxial growth of metals on metals with small lattice mismatch[10–12] or in reconstructed close-packed metal

surfaces such as Au(111) and Pt(111).[13] They have been shown to be suitable templates for the formation of metallic cluster arrays[14,15] and for site-selective adsorption of molecules.[16,17] In the following we demonstrate that the nanomesh corrugation acts like a chemical pattern for site-selective adsorption and immobilization of large molecules.

Naphthalocyanine (Nc) molecules were vapor-deposited onto the nanomesh kept at room temperature. These planar molecules have a diameter of about 2 nm and their size is therefore comparable to that of the nanomesh pores. The molecules form a well-ordered array with the periodicity of the nanomesh (3.22 nm), as shown in the STM images of Figure 2. High-resolution images reveal that individual Nc molecules are trapped inside the pores, which indicates highly site selective adsorption. Molecule/substrate interactions therefore dominate the adsorption behavior and intermolecular interactions are weak. This behavior is in contrast to Nc on flat graphite layers, where structure formation within the molecular layer is dominated by intermolecular interactions. A completely different pattern is observed in that case, with a much smaller periodicity of 1.7 nm.[18]

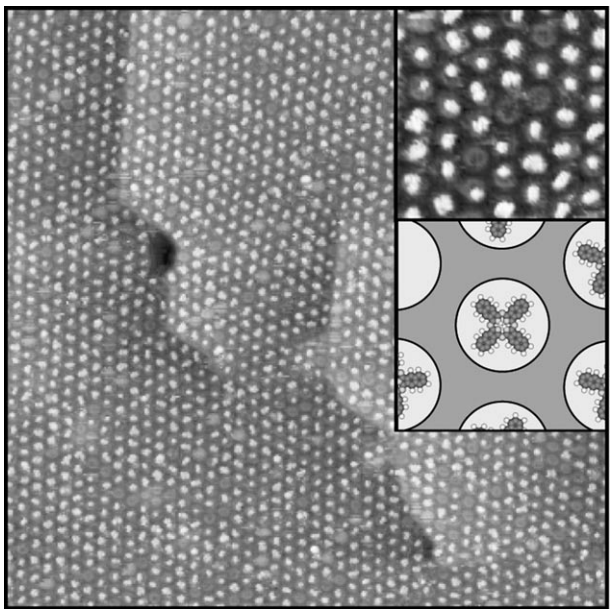

Figure 2. Site-selective adsorption in the nanomesh pores. STM image (120×120 nm^2, $I=0.3$ nA, $U=1.3$ V) showing a nearly complete monolayer[19] of Nc molecules on the nanomesh. The sample was annealed at $T=550$ K after deposition of the molecules. The inset on the top right shows an enlargement (19×19 nm^2) and gives a high-resolution view that shows trapping of the Nc molecules inside the nanomesh pores. The inset on the right shows a schematic representation of the molecular structure of naphthalocyanine ($C_{48}H_{26}N_8$) on top of a nanomesh pore.

The strength of the trapping potential for Nc was studied in time-lapsed STM series at partial coverage. At room temperature a very low mobility of the trapped molecules was observed with only rare hopping events: typically one out of a hundred molecules was found to have moved to a neighboring pore between two consecutive images, that is, within a time interval of about 200 s. Annealing experiments confirmed the rather high adsorption energy observed in STM. Annealing to 650 K does not lead to desorption of the molecules from the pores. Ultraviolet photoelectron spectroscopy (UPS) data (see Figure 3a) do not change after annealing to 550 and 650 K, and STM images also do not show a noticeable change in the coverage. The Nc molecules thus form a robust array of equally spaced and well-separated individual molecules on

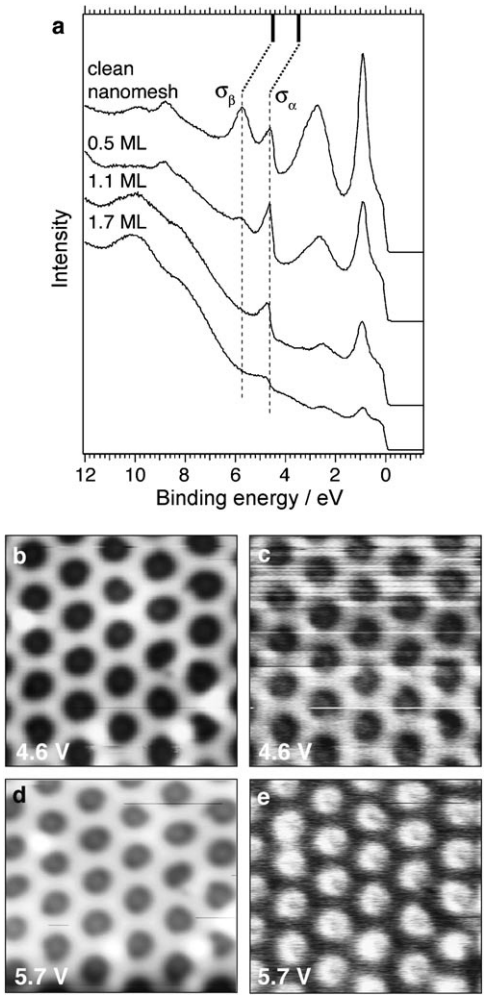

Figure 3. Electronic inequivalence of nanomesh wires and pores. a) Normal emission UPS spectra for increasing Nc coverages on the nanomesh. Site-selective adsorption of Nc is reflected in the selective attenuation up to the first monolayer (ML)[19] of the σ_β component that is associated with the nanomesh pores. Further increasing the coverage leads also to attenuation of the σ_α component that is related to the mesh wires. Spectral features at binding energies of 0–4 eV are dominated by the Rh substrate, those above 6 eV by the π bands of h-BN, and, for higher Nc coverages, by its molecular orbitals. The calculated eigenvalues (at the $\bar{\Gamma}$ point) for the σ band in the pores and on the wires are indicated by two vertical bars. The shift in absolute binding energy with respect to the UPS experiment is typical for DFT calculations. b) and d) Constant-current STM images (15×15 nm^2 and 15×13 nm^2) of the clean nanomesh measured at $I_t=0.1$ nA and sample bias voltages of $V_s=-4.6$ V and $V_s=-5.7$ V, respectively. Conductivity (dI/dV) maps recorded simultaneously with the topographic images in (b) and (d) are shown in (c) and (e). Map (c), measured at the voltage corresponding to the energy position of σ_α enhances the wires, while in (e), measured at the position of σ_β, the pores appear bright.

the nanomesh. The physical or chemical nature of the strong bonding and the trapping potential is the subject of current investigations.

Selective adsorption into the pores is also reflected in the normal emission UPS spectra (Figure 3). The spectrum of the clean h-BN layer on Rh(111) shows the appearance of two pairs of BN-related peaks and indicates the presence of two species of h-BN whose binding energies for the σ and π band are shifted by about 1 eV.[2] Adsorption of the molecules on the nanomesh leads to attenuation of the intensity of one of the σ-band components (σ_β) whereas the other (σ_α) remains unchanged for coverages up to one monolayer[19] (Figure 3a).

In the earlier double-layer nanomesh model, the component with higher binding energy, σ_β, was assigned to those parts of the mesh unit cell where either the top or the bottom layer is in direct contact with the underlying metal, while the component with lower binding energy, σ_α, was attributed to h-BN in the overlap region where it is separated from the metal by the first layer.[2] Complete attenuation of the σ_β component can only be rationalized with the new single-layer model. In concert with the STM images of Figure 2b, which show that the molecules cover the pores and not the mesh wires, these data prove unambiguously that this component is associated with the nanomesh pores, where the h-BN film is bonded to the substrate. It does not contain contributions from a second h-BN layer hidden below the mesh wires. In spite of its single-layer nature, the nanomesh remains an unusual structure and is distinct from a simple moiré pattern: in the case of h-BN on Pd(111), where the lattice mismatch is even larger than on Rh(111), STM images indicate a number of different, coexisting moiré patterns whereas the UPS spectrum shows a single σ and π component.[20]

Spectroscopic imaging of the nanomesh structure with STM gives the possibility to further investigate the nature of the two components. Conductivity or dI/dV maps were recorded by using a lock-in technique at 77 K simultaneously with constant-current topographic images, with an amplitude modulation of $V = 15$ mV at a frequency of 630 Hz. The contrast produced in such conductivity maps is dominated by the local density of electronic states (LDOS) at the binding energy defined by the bias voltage V_b. The data measured for $V_b = -5.7$ eV (Figure 3e), corresponding to the position of the σ_β component, clearly emphasize the nanomesh pores, while in the map measured at $V_b = -4.6$ eV (Figure 3c), that is, at the binding energy of σ_α, the LDOS is highest on the mesh wires. This contrast inversion in the dI/dV maps between the two bias voltages underlines the electronic inequivalence of pore and wire regions in the h-BN layer, which is in line with the split σ-band peak in the UPS spectra. The presence of two σ-band components is also reflected in the DFT calculations. Figure 3a shows the eigenvalues (at the $\bar{\Gamma}$ point) for the σ band obtained for local geometries corresponding to that in the pores and on the wires, and the splitting is in complete agreement with the experimental data.

In view of potential applications, an important requirement for a template meant for assembling molecular layers is its stability and its chemical inertness. The thermal stability of the nanomesh is inherently high due to its preparation temperature of 1050 K, and it has been further characterized up to 1275 K on Ru(0001).[4] It is stable in air,[3] and the chemical stability of the nanomesh has now been established also in liquid water and in perchloric acid. After immersion in the liquid, the nanomesh is clearly visible in STM images, although there is some remanent contamination on the surface (Figure 4).

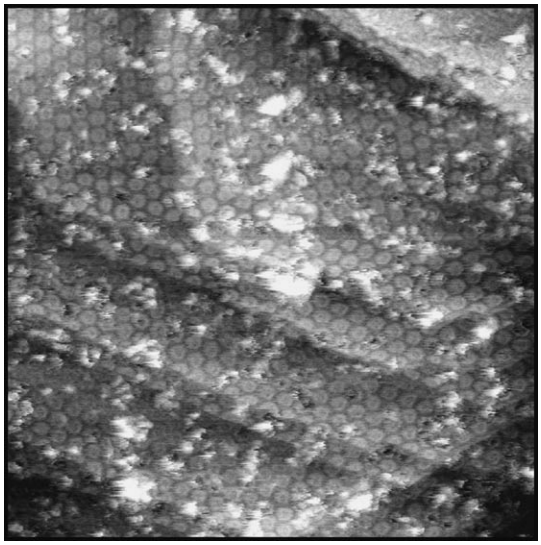

Figure 4. Stability of the nanomesh in aqueous solutions: STM image (80×80 nm^2, $I_t = 0.08$ nA, $V_s = -1$ V) of a h-BN nanomesh sample that was immersed for 30 min in ultrapure water before reinsertion into ultrahigh vacuum. Short annealing to 1025 K was applied to the sample before imaging. The nanomesh clearly survives this treatment.

In conclusion, the boron nitride nanomesh on Rh(111) surfaces has been identified as a single but corrugated monolayer of hexagonal boron nitride. The 2-nm-sized pores are formed by regions where the layer binds strongly to the underlying metal, while the regular hexagonal network of mesh wires represents regions where the layer is not bonded to the rhodium surface but only through strong cohesive forces within the film itself. The present study exemplifies the potential of the nanomesh as a template for the growth of stable and well-ordered molecular arrays. Wide spacing between individual molecules and negligible intermolecular interactions are in many cases mandatory for preserved functionality of individual molecules on surfaces. Such arrays might be interesting for applications such as molecular electronics and memory elements, in photochemistry, or in optical devices. The remarkable stability of a single h-BN monolayer on Rh(111) paves the way for applications of this material as a template that is not based on expensive ultrahigh vacuum deposition techniques, but on deposition from aqueous solutions.

Experimental Section

The h-BN nanomesh films were prepared with the recipe already presented elsewhere[2,4] on Rh(111) single crystals but also on single-crystalline Rh films with a typical thickness of 80–150 nm grown on Al_2O_3(0001). Exposure of the hot sample surface (1050 K) to

40 Langmuir (1 Langmuir = 10^{-6} torr s) of borazine leads to self-saturating formation of a well-ordered h-BN nanomesh layer covering the entire surface. STM images recorded at room temperature with tunneling currents around 1 nA and sample bias voltages close to −1 V give the impression of a hexagonal nanomesh with about 2-nm-wide pores, 1.2-nm-thick wires and a corrugation of 0.7 ± 0.2 Å.[2,4]

To investigate the stability of the h-BN nanomesh in aqueous environments, a nanomesh layer was grown on Rh(111)/Al_2O_3(0001) and removed from the ultrahigh-vacuum (UHV) system through a fast-entry air lock. The sample was then immersed for 30 min in ultrapure water and subsequently blow-dried in He. The dry sample was immediately reintroduced into the entry lock and slowly annealed up to 1025 K in UHV for outgassing. After this procedure, the nanomesh is clearly visible in STM images, although there is some remanent contamination on the surface (Figure 4). UPS spectra and low-energy electron diffraction (LEED) data confirm the presence of the h-BN nanomesh. In a similar experiment the nanomesh was immersed for 30 min in 0.01M perchloric acid and subsequently was rinsed in ultrapure water. After reintroduction into UHV and annealing, the presence of the nanomesh was again confirmed by STM, UPS, and LEED.

The growth of single-crystalline Rh(111) films is described in the Supporting Information.

Received: January 17, 2007
Revised: April 3, 2007
Published online: May 30, 2007

Keywords: boron · nanostructures · nitrides · scanning probe microscopy · self-assembly

[1] J. V. Barth, G. Costantini, K. Kern, *Nature* **2005**, *437*, 671.
[2] M. Corso, W. Auwärter, M. Muntwiler, A. Tamai, T. Greber, J. Osterwalder, *Science* **2004**, *303*, 217.
[3] O. Bunk, M. Corso, D. Martoccia, R. Herger, P. R. Willmott, B. D. Patterson, J. Osterwalder, J. F. van der Veen, T. Greber, *Surf. Sci.* **2007**, *601*, L7.
[4] A. Goriachko, Y. He, M. Knapp, H. Over, M. Corso, T. Brugger, S. Berner, J. Osterwalder, T. Greber, *Langmuir* **2007**, *23*, 2928.
[5] R. Laskowski, P. Blaha, T. Gallauner, K. Schwarz, *Phys. Rev. Lett.* **2007**, *98*, 106802.
[6] A. Nagashima, N. Tejima, Y. Gamou, M. Terai, C. Oshima, *Phys. Rev. B* **1995**, *51*, 4606.
[7] G. B. Grad, P. Blaha, K. Schwarz, W. Auwärter, T. Greber, *Phys. Rev. B* **2003**, *68*, 085404.
[8] The contrast and topography of the nanomesh as imaged by STM is strongly dependent on the particular tip as well as on the tunneling conditions. Sudden contrast reversals are observed sometimes during image acquisition due to spurious tip modifications.
[9] These images may indicate how the system relieves the considerable stress in the layer due to unfavorable positions of N and B atoms relative to the Rh(111) surface layer. However, the presence of the scanning tip could also lead to elastic surface relaxations, as observed in scanning force microscopy (R. Hoffmann, C. Barth, A. S. Foster, A. L. Shluger, H. J. Hug, H.-J. Güntherodt, R. M. Nieminen, M. Reichling, *J. Am. Chem. Soc.* **2005**, *127*, 17863). The h-BN layer is expected to be rather weakly, if at all, bonded to the substrate in the wire regions (see discussion in the text) and could therefore relax due to the interaction with the STM tip. This elastic relaxation could also give rise to the observed lattice distortions.
[10] H. Brune, H. Röder, C. Boragno, K. Kern, *Phys. Rev. B* **1994**, *49*, 2997.
[11] C. Günther, J. Vrijmoeth, R. Q. Hwang, R. J. Behm, *Phys. Rev. Lett.* **1995**, *74*, 754.
[12] J. Jacobsen, L. P. Nielsen, F. Besenbacher, I. Stensgaard, E. Lægsgaard, T. Rasmussen, K. W. Jacobsen, J. K. Nørskov, *Phys. Rev. Lett.* **1995**, *75*, 489.
[13] R. Pushpa, S. Narasimhan, *Phys. Rev. B* **2003**, *67*, 205418.
[14] H. Brune, M. Giovannini, K. Bormann, K. Kern, *Nature* **1998**, *394*, 451.
[15] N. Weiss, T. Cren, M. Epple, S. Rusponi, G. Baudot, S. Rohart, A. Tejeda, V. Repain, S. Rousset, P. Ohresser, F. Scheurer, P. Bencok, H. Brune, *Phys. Rev. Lett.* **2005**, *95*, 157204.
[16] M. Böhringer, K. Morgenstern, W.-D. Schneider, R. Berndt, F. Mauri, A. De Vita, R. Car, *Phys. Rev. Lett.* **1999**, *83*, 324.
[17] W. Xiao, P. Ruffieux, K. Aït-Mansour, O. Gröning, K. Palotas, W. A. Hofer, P. Gröning, R. Fasel, *J. Phys. Chem. B* **2006**, *110*, 21394.
[18] M. Lackinger, T. Müller, T. G. Gopakumar, F. Müller, M. Hietschold, G. W. Flynn, *J. Phys. Chem. B* **2004**, *108*, 2279.
[19] The term monolayer refers in this case to one Nc molecule per nanomesh pore.
[20] M. Morscher, M. Corso, T. Greber, J. Osterwalder, *Surf. Sci.* **2006**, *600*, 3280.

